Microstructure and mechanical properties of thermoelectric nanostructured n-type silicon-germanium alloys synthesized employing spark plasma sintering

Sivaiah Bathula, Bhasker Gahtori, M. Jayasimhadri, S. K. Tripathy, Kriti Tyagi, A. K. Srivastava, and Ajay Dhar

Citation: Applied Physics Letters **105**, 061902 (2014); doi: 10.1063/1.4892879

View online: http://dx.doi.org/10.1063/1.4892879

View Table of Contents: http://scitation.aip.org/content/aip/journal/apl/105/6?ver=pdfcov

Published by the AIP Publishing

Microstructure and mechanical properties of thermoelectric nanostructured n-type silicon-germanium alloys synthesized employing spark plasma sintering

Sivaiah Bathula,[1,2] Bhasker Gahtori,[1] M. Jayasimhadri,[2] S. K. Tripathy,[1] Kriti Tyagi,[1] A. K. Srivastava,[1] and Ajay Dhar[1,a)]
[1]*CSIR-Network of Institutes for Solar Energy, CSIR-National Physical Laboratory, Dr. K. S. Krishnan Marg, New Delhi 110012, India*
[2]*Department of Applied Physics, Delhi Technological University, Delhi, India*

(Received 25 June 2014; accepted 29 July 2014; published online 11 August 2014)

Owing to their high thermoelectric (TE) figure-of-merit, nanostructured $Si_{80}Ge_{20}$ alloys are evolving as a potential replacement for their bulk counterparts in designing efficient radio-isotope TE generators. However, as the mechanical properties of these alloys are equally important in order to avoid in-service catastrophic failure of their TE modules, we report the strength, hardness, fracture toughness, and thermal shock resistance of nanostructured n-type $Si_{80}Ge_{20}$ alloys synthesized employing spark plasma sintering of mechanically alloyed nanopowders of its constituent elements. These mechanical properties show a significant enhancement, which has been correlated with the microstructural features at nano-scale, delineated by transmission electron microscopy. © *2014 AIP Publishing LLC*. [http://dx.doi.org/10.1063/1.4892879]

Among the several available thermoelectric (TE) materials, SiGe alloys have been identified as one of the most important material for TE power generation, due to their high TE figure-of-merit (ZT), coupled with excellent thermal stability at high temperatures ~1000 °C.[1–3] For about the past four decades, SiGe based thermoelectrics have been used as TE devices for power generation in Radio-isotope TE Generators (RTG) for deep space missions.[4] In the recent past "nanostructuring" has resulted in significantly increasing the ZT of both n-type[5] and p-type[6] $Si_{80}Ge_{20}$ and thus nanostructured $Si_{80}Ge_{20}$ are evolving as a potential replacement for their conventional bulk counterparts in designing efficient RTGs.

A vast majority of the research done[1,5–8] on SiGe TE materials has been focused on their thermal and electrical transport properties primarily aimed towards enhancing their ZT. However, their mechanical properties are equally important for the long term reliability of their TE modules, as these materials are known to be brittle with low fracture toughness. In RTGs, the individual TE elements are subjected to significant stresses under in-service conditions, due to thermal cycling as well as thermal expansion mismatch and externally applied mechanical stresses. Thus, in order to ensure the structural reliability of SiGe TE modules, it becomes important that the material must withstand numerous mechanical vibrations and thermal stresses while in-service. Thus, apart from ZT, the mechanical properties of SiGe are equally vital in order to avoid catastrophic failure of their TE modules.

In the recent past, a high ZT in both n- and p-type nanostructured $Si_{80}Ge_{20}$ alloys has been reported by several researchers,[5,6,8,9] which is far higher than their bulk counterpart,[4] currently used for RTG applications. Owing to their enhanced TE performance, these nanostructured SiGe alloys are being seriously explored for their application in RTGs, replacing the conventional SiGe bulk alloys. However, in the literature there is no comprehensive reported data on a complete set of mechanical properties of these nanostructured alloys, although there have been some sporadic reports[3,10,11] about their hardness and fracture toughness.

With this premise, we report the detailed mechanical properties of nanostructured n-type $Si_{80}Ge_{20}$ alloys, synthesized employing the Spark Plasma Sintering (SPS) of mechanically alloyed $Si_{80}Ge_{20}$ nanopowders. The results suggest that these alloys exhibited superior mechanical properties compared to state-of-the-art TE materials in terms of toughness, and more importantly, thermal shock resistance. This increase in the fracture toughness has been explained on the basis of grain boundary sliding mechanism aided by the presence of soft amorphous phase at the grain boundaries,[12,13] which has been corroborated by High Resolution Transmission Electron Microscopy (HRTEM) results. Although the hardness and elastic modulus of the SiGe nanostructured alloy, synthesized in the present study, are comparable to those reported earlier,[10] but the fracture toughness was found to be significantly higher. Further, the thermal shock resistance of the nanostructured SiGe alloys, which has not been reported earlier, exhibited a very high value compared to other TE material.

Experimental procedure for synthesis and technique used for microstructural characterization of nanostructured n-type $Si_{80}Ge_{20}$ alloys has already been described in our earlier paper.[8] It may be noted that p-type nanostructured SiGe alloys can also be synthesized by similar method[8] employing SPS of mechanically milled elemental powders of Si and Ge doped with 1.2 at. % of Boron. The Fracture toughness measurements were carried out employing the indentation-crack technique using Vickers micro-hardness tester (FM-e7) with a load of 4.9 N for 10 s of indentation time. Elastic modulus and hardness were determined using nano-indentation

a)Author to whom correspondence should be addressed. Electronic mail: adhar@nplindia.org. Tel.: +91-11-45609456, Fax: +91-11-45609310.

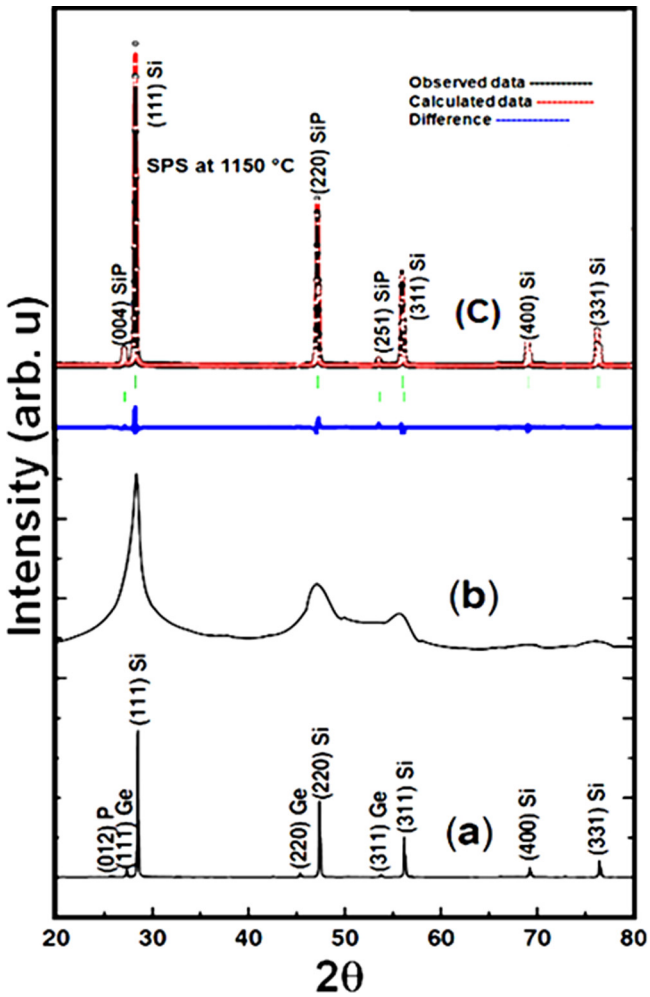

FIG. 1. X-ray powder diffraction patterns of $Si_{80}Ge_{20}$ alloy (a) unmilled powders, (b) nanopowders milled for 90 h, and (c) spark plasma sintered nanostructured alloy fitted with Rietveld refinement.

technique (M/s Fischer-Cripps, Australia) at a load of 10 mN and mechanical properties were derived from the measured load-penetration depth curves under loading/unloading through standard data analysis software. Compression tests were performed at room temperature as per ASTM standard (ASTM: E9–09) with an aspect ratio of ~2.5 under uni-axial loading with a strain rate of 2×10^{-5} s^{-1} (INSTRON 4204).

Fig. 1 elucidates the X-ray diffraction (XRD) patterns of unmilled powders, milled nanopowders, and after SPS of nanostructured $Si_{80}Ge_{20}$ alloy. The original average crystallite size of SiGe alloy powders was ~180 nm (Fig. 1(a)) and after 90 h of high energy ball milling the final crystallite size was found to be ~7 nm (Fig. 1(b)), calculated using XRD data employing Williamson-Hall method.[14] However, after SPS these crystallites slightly coarsened with an average crystallite size of ~12 nm (Fig. 1(c)). This suggests that the nano-scale features introduced during ball-milling are more-or-less retained post-sintering, which is primarily due to the high heating rates used during sintering.[8] However, Rietveld refinement of XRD data in Fig. 1(c) suggests the formation of an additional SiP phase (Fig. 2(d)) with an average crystallite size of ~4–6 nm.[8]

Fig. 2 shows the HRTEM images of nanostructured $Si_{80}Ge_{20}$ alloy. Fig. 2(a) shows a uniform microstructure with nanoscale crystallites, including some microstructural defects, which could be due to longer hours of ball-milling,[8,10,15] as shown in the inset. Further, at an atomic scale (Fig. 2(b)), an ultra-fine nano-grained microstructure with randomly oriented nanocrystallites (marked with dotted lines) with an average size of ~12 nm was delineated. Additionally, in Fig. 2(b) the presence of some amorphous region is also clearly visible. Fig. 2(c) shows the lattice scale image of nano-sized crystallite where the atomic planes hkl: 111 are marked. It can also be seen from this figure that, even at an atomic scale, the defects are clearly visible (region marked as "A").

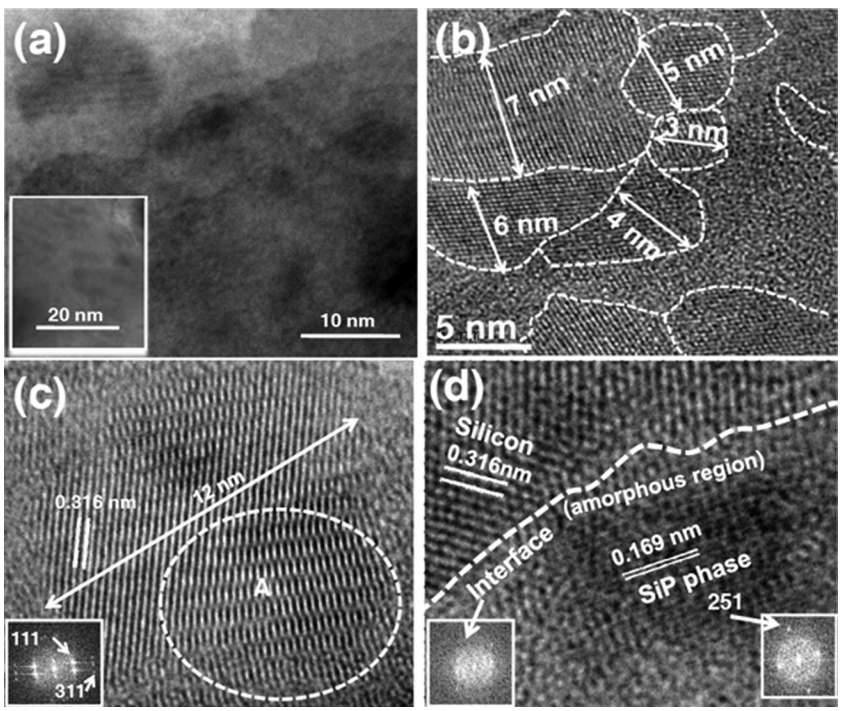

FIG. 2. HRTEM images of $Si_{80}Ge_{20}$ alloy showing (a) uniform ultra-fine densely packed microstructure, (b) distribution of different nano-grains marked with dotted white lines, and (c) a large sized nano-grain of about 12 nm with 0.316 nm inter-planar spacing and defect at lattice scale marked with dotted white line. Inset shows FFT of $Si_{80}Ge_{20}$ matrix showing the planes (111) and (311), (d) SiP phase with inter-planar spacing of 0.169 nm in the $Si_{80}Ge_{20}$ matrix. Inset shows the FFT of SiP phase showing the plane (251).

A corresponding fast Fourier transform (FFT) in reciprocal space shows the presence of the planes (hkl: 111 and 311) of Si (inset in Fig. 2(c)). SiP nano precipitates are also seen near the grain boundaries with a distribution of ~4–6 nm (Fig. 2(d)). The FFT of these nano-precipitates (inset in Fig. 2(d)) and the inter-planar spacing calculated in real space (0.169 nm) confirms that these nano-precipitates correspond to a SiP phase. Further, Figure 2(d) also clearly shows the presence of amorphous regions at the grain boundaries between the nanocrystallites and a hallow Debye ring in the corresponding FFT (inset in Fig. 2(d)) confirms this amorphous structure. Also, Fig. 3 clearly shows the amorphous nature of the grain boundaries (marked as regions A and B) between nano-crystallites of varying dimensions. A corresponding FFT in reciprocal space (inset of Fig. 3) further revealed that the 111 planes are randomly oriented and exhibit amorphous region at the grain boundaries and occurrence of these amorphous regions are well known in nanostructured materials,[16] including pristine Si[17] synthesized by mechanical alloying and is due to extended hours of ball milling.

Nanoindentation tests[18,19] were performed on the nanostructured $Si_{80}Ge_{20}$ alloy samples with a load of 10 mN using Berkovich[20] indenter with a face angle (θ) of 65.27°.[21] Fig. 4 shows the typical load-displacement nano-indentation curves. The elastic modulus (E) was determined from the slope of the unloading curve (dP/dh) and the depth of the contact circle (h_c) which is initial portion of this elastic unloading response at a maximum load (P_{max}),[18,21] which yielded a value 141 ± 2.3 GPa averaged over 10 indentations. Hardness values of nanoindentation test were derived from the indentation load divided by the projected contact area ($A = 3\sqrt{3}h_c^2\tan^2\theta$),[19] which exhibited a value of 13.7 ± 0.1 GPa. Earlier reports[10] on n-type $Si_{80}Ge_{20}$ alloys, exhibited a hardness of 12.4–14.7 GPa with an elastic modulus of 137–145 GPa, which is in reasonable agreement with our present results. However, the hardness is much higher in comparison to those reported for other TE materials, Bi_2Te_3 HV = 0.62 GPa,[22] LAST HV = 0.59–0.68 GPa,[23] PbTe HV = 0.23 GPa,[23] La_3Te_4 HV = 3.28–4.3 GPa,[24] and Skutterudites HV = 2.45–5.4 GPa.[24] The observed value of E, of our samples, was in reasonable good agreement with those reported earlier,[10] as it is well known that for bulk alloys the E is primarily a material composition dependent property, although it does slightly depend on porosity and other defects.[25]

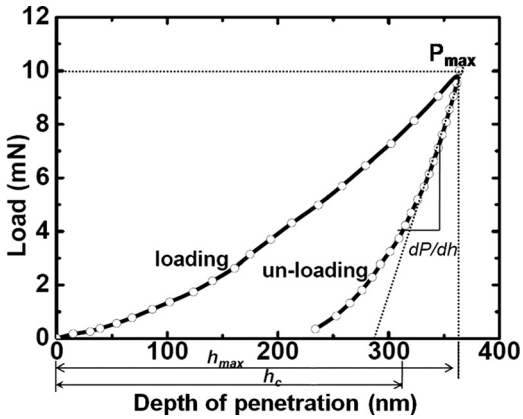

FIG. 4. Typical nanoindentation curves of nanostructured $Si_{80}Ge_{20}$ alloy during loading and un-loading.

Typical compressive stress-strain curve of nanostructured $Si_{80}Ge_{20}$ alloy as shown in Fig. 5 exhibits a strength of 1.18 ± 0.2 GPa with a strain at fracture of 6.34%. This high value of strength can be mainly associated with the strengthening due to grain refinement owing to a very small crystallite size,[13] solid-solution strengthening due to considerable difference in the atomic sizes of Si and Ge,[26,27] and strain hardening,[28] as these alloys are severely cold worked during high energy ball milling and there is always some residual strain,[27] even after sintering.[15,29] In comparison, other TE materials, such as, Skutterudite of composition $Ce_{0.5}Fe_{1.5}Co_{2.5}Sb_{12}$,[30] LAST, and LASTT[31] exhibit a compressive strength of ~1.80 GPa, 0.78–1.2 GPa, and 1.1 GPa, respectively.

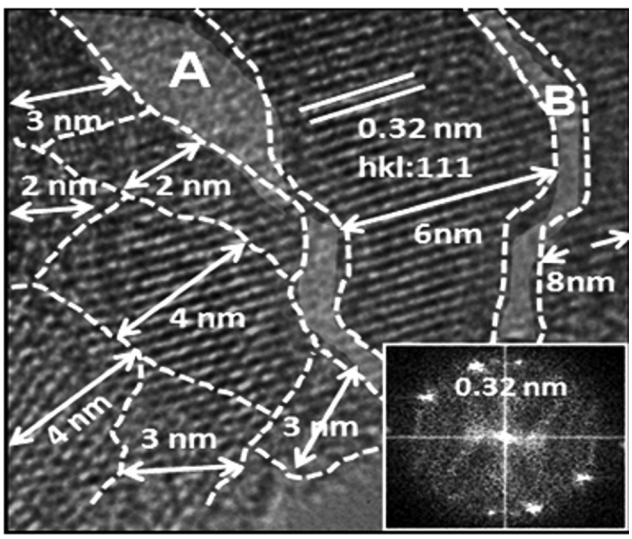

FIG. 3. HRTEM images of $Si_{80}Ge_{20}$ alloy, showing the distribution of different sized nano-crystallites with amorphous grain boundaries marked with white dotted lines marked as A and B. The inset shows the corresponding FFT in reciprocal space.

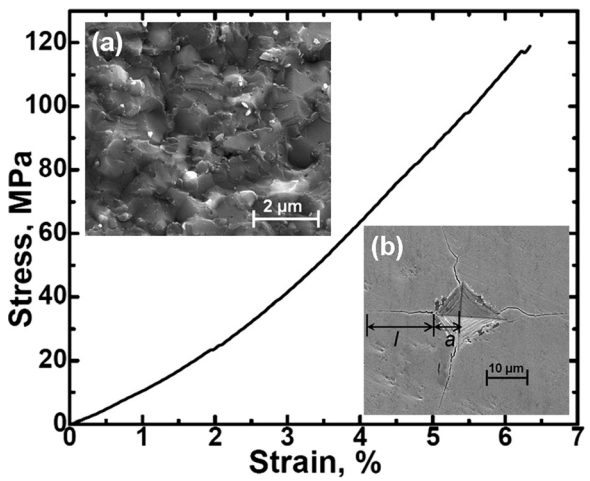

FIG. 5. Typical stress-strain curve of nanostructured $Si_{80}Ge_{20}$ alloy under uniaxial compression mode with a strain rate of 2×10^{-5} s^{-1}. Inset (a) FESEM image of fractured surface of nanostructured $Si_{80}Ge_{20}$ alloy and inset (b) FESEM images of Vickers-indentation crack developed at a load of 4.9 N. Indentation crack length (l) and the half-diagonal of Vickers indentation (a) are marked.

TABLE I. Mechanical properties of nanostructured n-type $Si_{80}Ge_{20}$ alloy.

Elastic modulus (GPa)	Hardness (GPa)	Compressive strength (GPa)	Fracture toughness ($MPam^{1/2}$)	Thermal shock resistance ($W\ m^{-1}$)
141 ± 2.3	13.7 ± 0.1	1.18 ± 0.2	1.6 ± 0.05	445 ± 18

The Field Emission Scanning Electron Microscope (FESEM) micrograph of the fractured surface of nanostructured n-type $Si_{80}Ge_{20}$ alloys is shown as an inset (a) of Fig. 5, which suggests that the fractured surface exhibits a mixed morphology of shallow ductile dimples intermingled with fractured cleavage surfaces (mixed modes of brittle and ductile fracture), which is also corroborated with enhanced fracture toughness.

The fracture toughness was estimated by a method proposed by Niihara *et al.*,[32] according to which the fracture toughness (K_{IC}), as measured by Vicker's indentation-crack technique with Palmqvist crack model,[33] is given as

$$K_{IC} = 0.0089\left(\frac{E}{H}\right)^{2/5} \times \frac{P}{al^{1/2}}, \quad 2.5 \geq \frac{l}{a} \geq 0.25, \qquad (1)$$

where P is the load in Newtons, l is the crack length on the material surface after indenter removal in meters, a is the half-diagonal of Vicker's indentation mark in meters, E is the Young's modulus in GPa, and H is the Vickers hardness in GPa. In the present work, dimensions a and l were measured using SEM for better accuracy of the results (inset (b) in Fig. 5). The calculated fracture toughness was found to be 1.6 ± 0.05 MPa $m^{1/2}$ and this is value ~60% higher than that reported for similar alloy composition.[10] It has also been recently reported[34,35] that in brittle materials the presence of amorphous phase at the grain boundaries helps to increase the fracture toughness as well as the strength, which is due to the grain boundary sliding assisted by the soft amorphous phase at the grain boundaries.[34] This situation is analogous to our nanostructured SiGe alloys, where the HRTEM microstructures (Figs. 2(d) and 3) shown a clear evidence of the presence of some amorphous phase at the grain boundaries, due to extended hours of ball milling. Thus, the enhancement of fracture toughness in nanostructured $Si_{80}Ge_{20}$ alloys could be attributed to grain boundary sliding,[36] which is easy to activate owing to the presence of soft amorphous phase at the grain boundaries, which can act as a lubricant to promote grain boundary sliding.[34] In comparison, other competing TE materials,[37] such as, Co_4Sb_{12} and $In_{0.1}Co_4Sb_{12}$ shown a fracture toughness of 0.82 ± 0.11 and 0.46 ± 0.13 $MPam^{1/2}$, respectively. Furthermore, even Bi_2Te_3 and LAST, which are state-of-the-art TE materials, have a reported fracture toughness of 1.15 and 0.34 $MPam^{1/2}$, respectively.[22,38]

Thermal Shock Resistance (R_T) is an important criterion for all the TE device material, but assumes special significance in the case of SiGe alloys as these are used in RTGs which have a very high operating temperatures ~900 °C. R_T is given by the expression[39]

$$R_T = \frac{\sigma(1-\nu)\kappa}{\alpha E}, \qquad (2)$$

where ν is the Poisson's ratio, κ is the thermal conductivity, and α is the coefficient of thermal expansion. The value of R_T for nanostructured $Si_{80}Ge_{20}$ alloy samples has been calculated using Eq. (2) by substituting the experimentally determined values of σ and E from the current study, κ from our earlier reported study[8] on nanostructured sample of identical composition and α[40] and ν[41] from the literature. The value of R_T of our nanostructured $Si_{80}Ge_{20}$ alloy sample was found to be $\sim 445 \pm 18$ W m^{-1}. This value is quite high in comparison to the reported values for other state-of-the-art high ZT TE materials[38] like, $Yb_{0.20}$ $Co_4Sb_{12.4}$ (Skutterudite) is 246 W m^{-1} and for PbTe is 140 W m^{-1}. The mechanical properties obtained in the present study, are summarized in Table I.

In summary, the nanostructured n-type $Si_{80}Ge_{20}$ alloy, synthesized using high energy ball milling followed by consolidation of resulting nanopowders employing SPS technique, resulted in an enhancement of their high mechanical properties. The nanostructured $Si_{80}Ge_{20}$ alloy exhibited a hardness of $\sim 13.7 \pm 0.1$ GPa with an elastic modulus of $\sim 141 \pm 2.3$ GPa and a compressive strength of 1.18 ± 0.2 GPa. This high value of strength can be mainly associated with strengthening due to grain refinement, solid-solution, and strain hardening strengthening mechanisms. Further, the fracture toughness found to be $\sim 1.60 \pm 0.05$ $MPam^{1/2}$ which is ~60% higher than best reported value for nanostructured alloy with similar composition. The increase in fracture toughness has been attributed to the grain boundary sliding mechanism, assisted by the soft amorphous phase at the grain boundaries. The thermal shock resistance exhibited a value of 445 ± 18 W m^{-1}, which is the highest reported value for any other TE material with ZT greater than unity. This combination of good mechanical properties coupled with high reported TE figure-of-merit makes nanostructured n-type $Si_{80}Ge_{20}$ a potential candidate for TE power generation for RTG applications.

This work was supported by CSIR-TAPSUN (CSIR-NWP-54) programme entitled "*Novel approaches for solar energy conversion under technologies and products for solar energy utilization through networking*." The technical support rendered by Dr. Sushil Kumar, Mr. Radhey Shyam, and Mr. Naval Kishor Upadhyay is gratefully acknowledged.

[1]C. B. Vining, J. Appl. Phys. **69**(1), 331 (1991).
[2]C. Wood, Rep. Prog. Phys. **51**(4), 459 (1988); D. M. Rowe, V. S. Shukla, and N. Savvides, Nature **290**, 765 (1981); B. Yu, M. Zebarjadi, H. Wang, K. Lukas, H. Wang, D. Wang, C. Opeil, M. Dresselhaus, G. Chen, and Z. Ren, Nano Lett. **12**(4), 2077 (2012).
[3]D. M. Rowe and V. S. Shukla, J. Appl. Phys. **52**(12), 7421 (1981).
[4]D. M. Rowe, *CRC Handbook of Thermoelectrics* (CRC press, 1995).
[5]X. W. Wang, H. Lee, Y. C. Lan, G. H. Zhu, G. Joshi, D. Z. Wang, J. Yang, A. J. Muto, M. Y. Tang, and J. Klatsky, Appl. Phys. Lett. **93**(19), 193121 (2008).
[6]G. Joshi, H. Lee, Y. Lan, X. Wang, G. Zhu, D. Wang, R. W Gould, D. C. Cuff, M. Y. Tang, and M. S. Dresselhaus, Nano Lett. **8**(12), 4670 (2008).

[7]J. Yang, H.-L. Yip, and A. K.-Y. Jen, Adv. Energy Mater. **3**(5), 549 (2013); H. Lee, D. Vashaee, D. Z. Wang, M. S. Dresselhaus, Z. F. Ren, and G. Chen, J. Appl. Phys. **107**(9), 094308 (2010).
[8]S. Bathula, M. Jayasimhadri, N. Singh, A. K. Srivastava, J. Pulikkotil, A. Dhar, and R. C. Budhani, Appl. Phys. Lett. **101**(21), 213902 (2012).
[9]H. Yin, M. Christensen, N. Lock, and B. B. Iversen, Appl. Phys Lett. **101**(4), 043901 (2012).
[10]A. C. Kallel, G. Roux, and C. L. Martin, Mater. Sci. Eng., A **564**, 65 (2013).
[11]F. Ericson, S. Johansson, and J.-Å. Schweitz, Mater. Sci. Eng., A **105**, 131 (1988).
[12]C. C. Koch, Nanostruct. Mater. **9**(1), 13 (1997); M. Gust, G. Goo, J. Wolfenstine, and M. L. Mecartney, J. Am. Ceram. Soc. **76**(7), 1681 (1993).
[13]A. A. Voevodin and J. S. Zabinski, Compos. Sci. Technol. **65**(5), 741 (2005).
[14]B. D. Cullity, *Prentice Hall* (New Jersey, USA, 2001).
[15]S. Bathula, R. C. Anandani, A. Dhar, and A. K. Srivastava, Mater. Sci. Eng., A **545**, 97 (2012).
[16]J.-F. Li, W.-S. Liu, L.-D. Zhao, and M. Zhou, NPG Asia Mater. **2**(4), 152 (2010); A. I. Hochbaum, R. Chen, R. Diaz Delgado, W. Liang, E. C. Garnett, M. Najarian, A. Majumdar, and P. Yang, Nature **451**(7175), 163 (2008).
[17]J. Tang, H.-T. Wang, D. H. Lee, M. Fardy, Z. Huo, T. P. Russell, and P. Yang, Nano Lett. **10**(10), 4279 (2010).
[18]B. Lawn, *Fracture of Brittle Solids* (Cambridge University Press, 1993).
[19]W. C. Oliver and G. M. Pharr, J. Mater. Res. **19**(1), 3 (2004).
[20]E. S. Berkovich, Ind. Diamond Rev. **11**(127), 129 (1951).
[21]A. C. Fischer-Cripps, *Nanoindentation* (Springer, 2011).
[22]L.-D. Zhao, B.-P. Zhang, J.-F. Li, M. Zhou, W.-S. Liu, and J. Liu, J. Alloys Compd. **455**(1), 259 (2008).
[23]F. Ren, E. D. Case, E. J. Timm, and H. J. Schock, J. Alloys Compd. **455**(1), 340 (2008).
[24]J. M. Ma, S. A. Firdosy, R. B. Kaner, J.-P. Fleurial, and V. A. Ravi, J. Mater. Sci. **49**(3), 1150 (2014).
[25]J. R. Gladden, G. Li, R. Adebisi, S. Firdosy, T. Caillat, and V. Ravi, Phys. Rev. B **82**(4), 045209 (2010); F. Ren, E. D. Case, E. J. Timm, and H. J. Schock, Philos. Mag. **87**(31), 4907 (2007).
[26]C. Suryanarayana, E. Ivanov, and V. V. Boldyrev, Mater. Sci. Eng., A **304**, 151 (2001); T.-Y. Chiang, H.-C. Wen, W.-C. Chou, and C.-H. Tsai, J. Cryst. Growth **390**, 92 (2014).
[27]J. Schilz, K. Pixius, W. Wunderlich, and W. A. Kaysser, Appl. Phys. Lett. **66**(15), 1903 (1995).
[28]P. B. Littlewood, Phys. Rev. B **34**(2), 1363 (1986).
[29]K. Biswas, A. Mukhopadhyay, B. Basu, and K. Chattopadhyay, J. Mater. Res. **22**(06), 1491 (2007).
[30]P. C. Zhai, W. Y. Zhao, Y. Li, L. S. Liu, X. F. Tang, Q. J. Zhang, and M. Niino, Appl. Phys. Lett. **89**(5), 052111 (2006).
[31]J. E. Ni, F. Ren, E. D. Case, and E. J. Timm, Mater. Chem. Phys. **118**(2), 459 (2009).
[32]K. Niihara, R. Morena, and D. P. H. Hasselman, J. Mater. Sci. Lett. **1**(1), 13 (1982).
[33]S. Palmqvist, Jernkontorets Ann. **141**, 300 (1957).
[34]W. J. MoberlyChan, J. J. Cao, and L. C. De Jonghe, Acta Mater. **46**(5), 1625 (1998).
[35]D. Chen, M. E. Sixta, X. F. Zhang, L. C. De Jonghe, and R. O. Ritchie, Acta Mater. **48**(18), 4599 (2000); H.-J. Kleebe, G. Pezzotti, and G. Ziegler, J. Am. Ceram. Soc. **82**(7), 1857 (1999).
[36]K. Madhav Reddy, P. Liu, A. Hirata, T. Fujita, and M. W. Chen, Nat. Commun. **4**, 2483 (2013).
[37]J. Eilertsen, M. A. Subramanian, and J. J. Kruzic, J. Alloys Compd. **552**, 492 (2013).
[38]J. R. Salvador, J. Yang, X. Shi, H. Wang, A. A. Wereszczak, H. Kong, and C. Uher, Philos. Mag. **89**(19), 1517 (2009).
[39]J. R. Salvador, J. Yang, A. A. Wereszczak, H. Wang, and J. Y. Cho, Sci. Adv. Mater. **3**(4), 577 (2011).
[40]F. Schaffler, *Properties of Advanced Semiconductor Materials GaN, AlN, InN, BN, SiC, SiGe*, edited by M. E. Levinshtein, S. L. Rumyantsev, and M. S. Shur (John Wiley & Sons, Inc., New York, 2001), p. 149.
[41]J. J. Wortman and R. A. Evans, J. Appl. Phys. **36**(1), 153 (1965).